Nitrous oxide production in intermittently aerated Partial Nitritation-Anammox reactor: oxic N_2O production dominates and relates with ammonia removal rate

Blum, Jan-Michael; Jensen, Marlene Mark; Smets, Barth F.

Published in:
Chemical Engineering Journal

Link to article, DOI:
10.1016/j.cej.2017.10.146

Publication date:
2018

Document Version
Peer reviewed version

Citation (APA):
Blum, J-M., Jensen, M. M., & Smets, B. F. (2018). Nitrous oxide production in intermittently aerated Partial Nitritation-Anammox reactor: oxic N_2O production dominates and relates with ammonia removal rate. *Chemical Engineering Journal*, *335*, 458-466. https://doi.org/10.1016/j.cej.2017.10.146

Title

Nitrous oxide production in intermittently aerated Partial Nitritation-Anammox reactor: oxic N_2O production dominates and relates with ammonia removal rate.

Authors

Jan-Michael Blum[a], Marlene Mark Jensen[a], Barth F. Smets[a]*

Affiliation: [a] Department of Environmental Engineering, Technical University of Denmark, Miljøvej Building 113, 2800 Kongens Lyngby, Denmark

*corresponding author: E-Mail: bfsm@env.dtu.dk (Barth F. Smets)

Abstract

Emissions of the greenhouse gas nitrous oxide from the Partial Nitritation-Anammox process are of concern and can determine the carbon footprint of the process. In order to reduce nitrous oxide emissions intermittent aeration regimes have been shown to be a promising mode of operation, possibly due to an effective control of accumulation of nitrogen intermediates. However, due to frequent changes of redox conditions under intermittent aeration regimes, nitrous oxide production and emissions are dynamic. In this study the production and emission dynamics of nitrous oxide in an intermittently aerated sequencing batch reactor were monitored in high temporal resolution, the contribution of different redox conditions to overall nitrous oxide production was quantified and the most relevant factors for nitrous oxide production were identified. The average fraction of nitrous oxide produced (per unit ammonium removed) was 1.1±0.5%. Cycle-averaged approx. 80% of nitrous oxide was produced during aerated phases, the remaining 20% were produced during non-aerated phases. Yet, the intra-cycle dynamics of nitrous oxide were substantial. The net-production rate of nitrous oxide during aerated phases correlated with the ammonia removal rate, whereas the concentration of nitrite determined the production during non-aerated phases. While aerated phases contributed predominantly at the beginning of reactor cycles, non-aerated phases became the dominant source of nitrous oxide at the end. Particularly low net-production rates were observed at ammonia removal rates below 5 mg NH_3-N*$gVSS^{-1}$*L^{-1}, when the fraction of nitrous oxide produced was 0.011±0.004% (per ammonia removed). Based on the nitrous oxide dynamics and correlations, reactor operation at relatively low nitrogen loadings (below 100 mg NH_4^+-N*L^{-1}), ammonia removal rates of approx. 5 mg NH_3-N*$gVSS^{-1}$*L^{-1} and nitrite concentrations below 1 mg NO_2^-N*L^{-1} appears as beneficial for low emission of nitrous oxide.

Keywords

aerobic granules, nitrogen removal, biofilm, anammox, nitrous oxide

1. Introduction

The removal of ammonium (NH_4^+) from municipal wastewater streams is essential to protect receiving water bodies from eutrophication. One process to accomplish this task is the Partial Nitritation-Anammox (PNA) process [1]. To date, most PNA processes are applied in the treatment of NH_4^+-rich water streams at mesophilic temperatures (sidestream). Essentially, the PNA process consists of two biological conversion steps, a) Partial Nitritation (PN) and b) anaerobic ammonium oxidation (anammox). During PN NH_4^+ is converted aerobically to nitrite (NO_2^-) by ammonia oxidizing bacteria (AOB). During anammox NH_4^+ is, together with NO_2^-, converted anaerobically to the desired product dinitrogen gas (N_2) by anammox bacteria (AnAOB) [2]. PNA can be obtained via single-stage (one reactor) or two-stage (two reactors) operation. The majority (88% in 2014) of full-scale applications are single-stage systems in which AOB and AnAOB co-exist in bio-granules to metabolize NH_4^+ to environmentally inert dinitrogen gas (N_2) [1,3]. Both continuous and

intermittent aeration strategies have been implemented in PNA systems to achieve efficient NH_4^+ removal [3]: While some studies show stable operation under continuous aeration [4], others find increased performance under intermittent aeration regimes and claim benefits of periodic anoxic phases for community metabolism, the suppression of undesired microbial groups (e.g. NOB) and energy savings due to a reduction of overall aeration time [5,6].

Emissions of nitrous oxide (N_2O) from PNA systems are of concern, as N_2O is an ozone depleting agent and a potent greenhouse gas with a global warming potential (GWP_{100}) of 298 [7]. Due to its large GWP_{100}, already low amounts of emitted N_2O can substantially contribute to the carbon footprint of PNA [8]. A better understanding of the biological turnover processes of nitrogen compounds during PNA and relevant parameters for the mitigation of N_2O emissions are needed to improve process sustainability.

Nitrous oxide originates mainly from three biochemical pathways during PNA [2,9–12]: 1) In the hydroxylamine oxidation pathway (HO), N_2O is produced by AOB during the oxidation of hydroxylamine (NH_2OH), 2) in the nitrifier denitrification (ND) pathway, N_2O is produced by AOB during the reduction of NO_2^-, and 3) during anaerobic reduction of NO_2^- and NO_3^- by heterotrophic denitrification (HD), N_2O is produced as an intermediate before the final reduction to N_2 [10]. N_2O produced during anammox is considered negligible [13].

The contribution of the different pathways to the total N_2O production depends on the activity of different microbial groups and varies with process conditions, e.g. concentration of NH_4^+, NO_2^-, DO and pH [2,14,15]. The production of N_2O by HO increases at high ammonia removal rates (AOR) and NH_4^+ concentrations [16], whereas N_2O production by ND is favored at high NO_2^- and low DO concentrations [14,17]. The availability of organic carbon is critical for the contribution of HD, and HD can become the dominant N_2O production pathway under stoichiometric sub-optimal carbon loadings [11].

Dynamics of N_2O production in PNA systems have been investigated in intermittently aerated and continuously-fed reactors [4,18] and also in continuously aerated sequencing batch reactors (SBRs) [8,19]. Yet, few studies have investigated the dynamics of N_2O production in intermittently aerated SBRs, which potentially combine the advantages of SBRs, e.g. high volumetric loading rates and low effluent concentrations, with advantages of intermittent aeration regimes, e.g. control of accumulation of N-intermediates and potential reduction of aeration energy [20,21]. In an earlier study, N_2O production was reduced in a PNA SBR at high frequencies of aeration intermittency [20]. The authors speculated that a decline in net-N_2O production rates at high aeration frequency was probably caused by lower transient NO_2^- accumulation and lower AORs. However, AORs were determined by extant AOB activity assays, which likely overestimated AOB activity.

This study monitored the AORs and N_2O dynamics of an intermittently aerated PNA SBR at a high temporal resolution. The combination of intermittent aeration and continuous stripping experiments together with N_2O micro-sensor measurements and off-gas N_2O analysis on a short time scale allowed an unique quantification of the contribution of different redox conditions to the overall N_2O production and enabled an in depth analysis of the effect of AORs and NO_2^- on net-N_2O production. To study the contribution of different redox conditions, AORs and NO_2^- concentrations we designed a series of experiments a) to identify the main phases of N_2O production during SBR cycles, b) to correlate the N_2O production with process parameters, c) to examine the effect of fluctuating pH as

a driver for N_2O dynamics and d) to assess the potential contribution of heterotrophic bacteria to N_2O production.

2. Material and Methods

2.1. Reactor operation

A 4L lab-scale reactor (Biostat A Plus, Sartorius, Göttingen, DE) was operated as an intermittently aerated sequencing batch reactor. Temperature was controlled at 30°C. The reactor was inoculated with biomass from a carrier based PNA pilot plant (AnoxKaldnes™, Sweden). Biomass was scraped off the carriers before transfer to the reactor. The reactor was fed with synthetic digester liquor medium, which was based on van de Graaf et al. [22] and contained per 1 L deionized water: 1694 mg NH_4HCO_3 (= 300 mg NH_4-N/L), 360 mg $NaHCO_3$ (CO_3^{2-}:NH_4^+ = 1.2), 170 mg KH_2PO_4 (1.25 mM), 750 mg $MgSO_4*7H_2O$ (3.05 mM), 450 mg $CaCl_2*2H_2O$ (3.07 mM), 10 mg $FeSO_4*7H_2O$ (36 µM), 10 mg EDTA (34 µM), 4 mg EDTA-Na_2 (11 µM), 0.43 mg $ZnSO_4*7H_2O$ (1.5 µM), 0.24 mg $CoCl_2*6H_2O$ (1 µM), 1 mg $MnCl_2*4H_2O$ (5 µM), 0.25 mg $CuSO_4*5H_2O$ (1 µM), 0.24 mg $NaMoO_4*2H_2O$ (1 µM), 0.19 mg $NiCl_2*6H_2O$ (0.80 µM), 0.2 mg $NaSeO_4*10H_2O$ (0.57 µM). The daily reactor load was 900 mg NH_4-N L^{-1} d^{-1}. One SBR cycle included a feeding phase (t_{feed}), reaction phase (t_{react}), settling phase (t_{settle}) and effluent phase ($t_{effluent}$) (nomenclature adapted from [23]). For experiments 1 and 3, a long cycle configuration was applied (Table 1). For experiment 2, a short cycle configuration was applied. The short cycle mimicked the last third of the long cycle operation. During t_{react} aeration was switched on and off 15 times (f_{redox}=15) with each aerated and non-aerated phase lasting for 15 minutes. For the short cycle configuration, f_{redox} was 5. The length of aerated/non-aerated phases was fixed and guaranteed a full depletion of NO_2^- during non-aerated phases to prevent accumulation of NO_2^- over cycle time. Air was supplied at Q_{air}= 2.0 L min^{-1} during aerated phases through a diffuser at the bottom of the reactor. Stirring took place with 80 rpm during t_{feed} and t_{react} and was stopped during t_{settle} and $t_{effluent}$.

Table 1 - Key parameters of long and short cycle operation of SBR.

		configuration	
		long cycle	short cycle
	t_{cycle} [min]	480	160
phase	t_{feed}	10	2
	t_{react}	450	150
	t_{settle}	13.5	5.5
	$t_{effluent}$	6.5	2.5
	f_{redox}	15	5
	T [°C]	30	30
	pH	7-8	7
	HRT [hr]	16	16
	V_{ex} [%]	50	17
N-load	[mg NH_4^+-N*L^{-1}*$cycle^{-1}$]	300	100
	[mg NH_4^+-N*L^{-1}*d^{-1}]	900	900
N-species monitored	NH_4^+-N	yes	yes
	NO_2^--N	no	yes
	NO_3^--N	yes	yes
	$N_2O_{(g)}$	yes	yes
	$N_2O_{(aq)}$	no	yes

2.2. Process control & monitoring

The SBR was controlled by a digital control unit (Sartorius, Göttingen, DE), which itself was accessed by a customized LabView (National Instruments, Austin, US) protocol to manage cycle operation. Temperature, pH and DO were monitored continuously (every 10 seconds) using a Pt-100 temperature sensor, an EasyFerm plus K8 pH electrode (Hamilton, Bonaduz, CH) and an OxyFerm 235 FDA DO electrode (Hamilton, Bonaduz, CH), respectively. Air flow was controlled by an EL-FLOW mass-flow controller, which was regulated by FlowDDE software (Bronkhorst, Ruurlo, NL).

2.3. Monitoring of N-species

2.3.1. NH_4^+, NO_3^- and NO_2^-

Bulk NH_4-N and NO_3-N concentrations were measured every minute by Varion Plus 700IQ ion-selective electrodes (WTW, Weilheim, DE).

Grab samples for NO_2^- measurements were filtered (0.2 µm) before measurement. NO_2^- concentrations were determined by a colorimetric assay based on sulphanilamide and N-(1-naphtyl)-ethylenediamine dihydrochloride with absorbance measurement at 540 nm in a 96 well plate reader (Synergy Mx, BioTek, Winooski, US) (adapted from [24]).

2.3.2. N_2O

The N_2O concentration in the reactor off-gas was measured and logged every minute with a gas filter correlation N_2O analyzer (Teledyne API, San Diego, CA, US). The off-gas N_2O analyzer collected off-gas at a constant rate of 0.4 $L*min^{-1}$ from the headspace of the reactor. Calibration was performed after manufacturer's instruction with 200 ppm N_2O in N_2 as span gas and N_2 as zero gas.

The N_2O concentration in the bulk liquid was measured every 30 seconds by a N_2O-R micro-sensor (Unisense, DK). Calibration was performed in biomass free medium with spikes of saturated N_2O solution after manufacturer's instruction.

2.4. Particle size analysis

15 ml mixed liquor samples were withdrawn in an aerated phase (maximum turbidity) at three different positions of the reactor (top, middle, bottom), 5 ml each. The samples were pooled and triplicate particle size measurements were performed in a Mastersizer 2000 laser diffractometer equipped with a liquid sample loading and dispersion unit (Malvern Instruments Ltd., Malvern, UK). The refraction index was set to 1.5.

2.5. DNA extraction and quantitative PCR (qPCR)

To quantify the abundance of bacteria involved in the nitrogen transformations, triplicate biomass samples were taken in the first aerated phase of SBR cycles. DNA was extracted from 3 mg of biomass (dry weight) using a Fast DNA™ SPIN Kit for soils (MP Biomedicals, USA) according to manufacturer's instruction. The quantity and quality of extracted DNA was measured and checked by its 260/280 ratio with NanoDrop (ThermoFisher Scientific, Rockwood, TN, USA). DNA was stored at -80°C before further analysis. Biomass sampled during experiment 1 was subject to qPCR analysis. The relative abundance of ammonia oxidizing bacteria, anammox bacteria, nitrite oxidizing bacteria and total bacteria was determined based on 16S rRNA genes, following the procedure by [25]. Primers and conditions for quantification of each target organism are listed in Table 2.

Table 2 - Primers and conditions used for the quantification of bacterial numbers by qPCR based on 16S rRNA.

Target Organism	Primers	Sequence (5´-3´)	Annealing Temp.	Reference
All Bacteria	1055f 1392r	ATG GCT GTC GTC AGC T ACG GGC GGT GTG TAC	55	[26,27]
β-proteobacterial AOB	CTO189fa/b CTO189fc RT1r	GGA GRA AAG CAG GGG ATC G GGA GGA AAG TAG GGG ATC G CGT CCT CTC AGA CCA RCT ACT G	60	[28,29]
NOB *Nitrobacter*	FGPS872f FGP1269r	CTA AAA CTC AAA GGA ATT GA TTT TTT GAG ATT TGC TAG	50	[30]
NOB *Nitrospira*	Nspra675f Nspra746r	GCG GTG AAA TGC GTA GAK ATC G TCA GCG TCA GRW AYG TTC CAG AG	58	[31]
Anammox	Amx809f Amx1066r	GCC GTA AAC GAT GGG CAC T AACGTCTCACGACACGAGCTG	67	[32]

2.6. Experimental Design

The experiments of the study are summarized in Table 3.

Table 3 – Summary of experimental design and objective of experiments

experiment	configuration	feature	objective
1 a	long cycle	standard operation	detailed monitoring of N_2O emissions over the course of SBR cycles
b	long cycle	continuous sparging of gas results in continuous supply of gas to off-gas N_2O analyzer	insights into non-aerated phases with off-gas N_2O analyzer
2	short cycle	constant pH, pH = 7.0	monitoring of N_2O production at constant pH for comparison with fluctuating pH in exp. 1
3	long cycle	stop of aeration after ½*t_{cycle}, operation under anoxic condition for 275 min.	assessment of activity of heterotrophic denitrifiers

2.6.1. Experiment 1: Analysis of temporal dynamics of N_2O production and emission during SBR cycle

Experiment 1 was designed to monitor the N_2O emissions during a SBR cycle in order to analyze the off-gas N_2O profile in respect to other measured process parameters (pH, concentration profiles of N-species, DO, aerated/non-aerated phases). The SBR was operated under long cycle configuration, as described in 2.1. Due to the nature of the aeration regime, i.e. flow of gas during aerated phases and no flow of gas during non-aerated phases, no information about N_2O production is available from the off-gas analyzer in the non-aerated phases. Therefore, we measured one additional cycle of experiment 1 with a constant flow of gas throughout t_{react} and supplied N_2 gas at a flow rate of Q_{N2} = 2 L*min^{-1} during non-aerated phases. Consequently, $N_2O_{(aq)}$ was stripped at approx. the same rate during both aerated and non-aerated phases. Thus, information on the N_2O production dynamics during non-aerated phases was available from the off-gas N_2O analyzer. Due to constant stripping, it was assumed that N_2O emitted ≈ N_2O produced. Yet, we define the reactor operation without constant stripping as our reference condition, as it reflects more realistically how a full-scale SBR would be operated. We will refer to the measurement under standard operation with intermittent aeration as experiment 1.a. The measurements with constant flow of gas during t_{react}, is termed experiment 1.b.

2.6.2. Experiment 2: N_2O emission profile at constant pH

The pH during a SBR cycle under standard operation fluctuated. To differentiate between a potential effect of pH (H^+ concentration) and the effect of varying NH_4^+/NH_3 concentrations on N_2O emissions (also as a result of varying pH), the system was operated at constant pH of 7.0 during experiment 2. The NH_4^+ source was changed from ammonium bicarbonate to ammonium chloride. Aliquots of concentrated sodium bicarbonate (83 g $NaHCO_3$*L^{-1}) were added to maintain pH. The cycle was operated at short cycle configuration. In comparison to experiment 1 and 3, in

experiment 2 additionally bulk liquid N_2O were measured in situ (see 2.3.2.) (micro-sensor, Unisense, DK) and NO_2^- concentrations were obtained from grab-samples (see 2.3.1.)

2.6.3. Experiment 3: Assessment of heterotrophic denitrification activity

Although the system was only fed with carbonate as carbon source, activity of heterotrophic bacteria was likely. To assess their potential activity, the reactor was operated for four hours under anoxic conditions (as in experiment 1 under long cycle configuration, with the exception that aeration was stopped at t=205 min.). The reactor remained under anoxic conditions with excess of NH_4^+ and NO_3^- for 275 minutes. The NO_3^- removal rate was used as an indicator of the activity of heterotrophic denitrifiers.

3. Results

3.1. System performance

System performance was stable for 3 month prior to the N_2O measurement campaign. Biomass concentration was 1.8±0.1 gVSS/L at a median diameter of bio-granules of approx. 275 µm during the measurement campaign (Fig.SI.1 in Supplementary Material). The microbial community was composed of ~18% AOB, ~30% AnAOB, <0.2% NOB and ~52% other bacteria (Fig.SI.2 in Supplementary Material). Under standard operation 300±3 mg NH_4^+-N/L per cycle were removed with almost 99% removal efficiency (Fig. 1). Total N-removal efficiency was 89%. The effluent concentrations of NH_4^+-N, NO_2^--N and NO_3^--N were 4.1±0.6 mg NH_4^+-N/L, 0.7±0.7 NO_2^--N/L and 75.4±2.8 mg NO_3^--N/L. The fraction of N_2O emitted per NH_4^+ removed was 1.1±0.5%. The average NH_4^+ removal rate was 23.9±2.6 mg NH_4^+-N*gVSS^{-1}*h^{-1}.

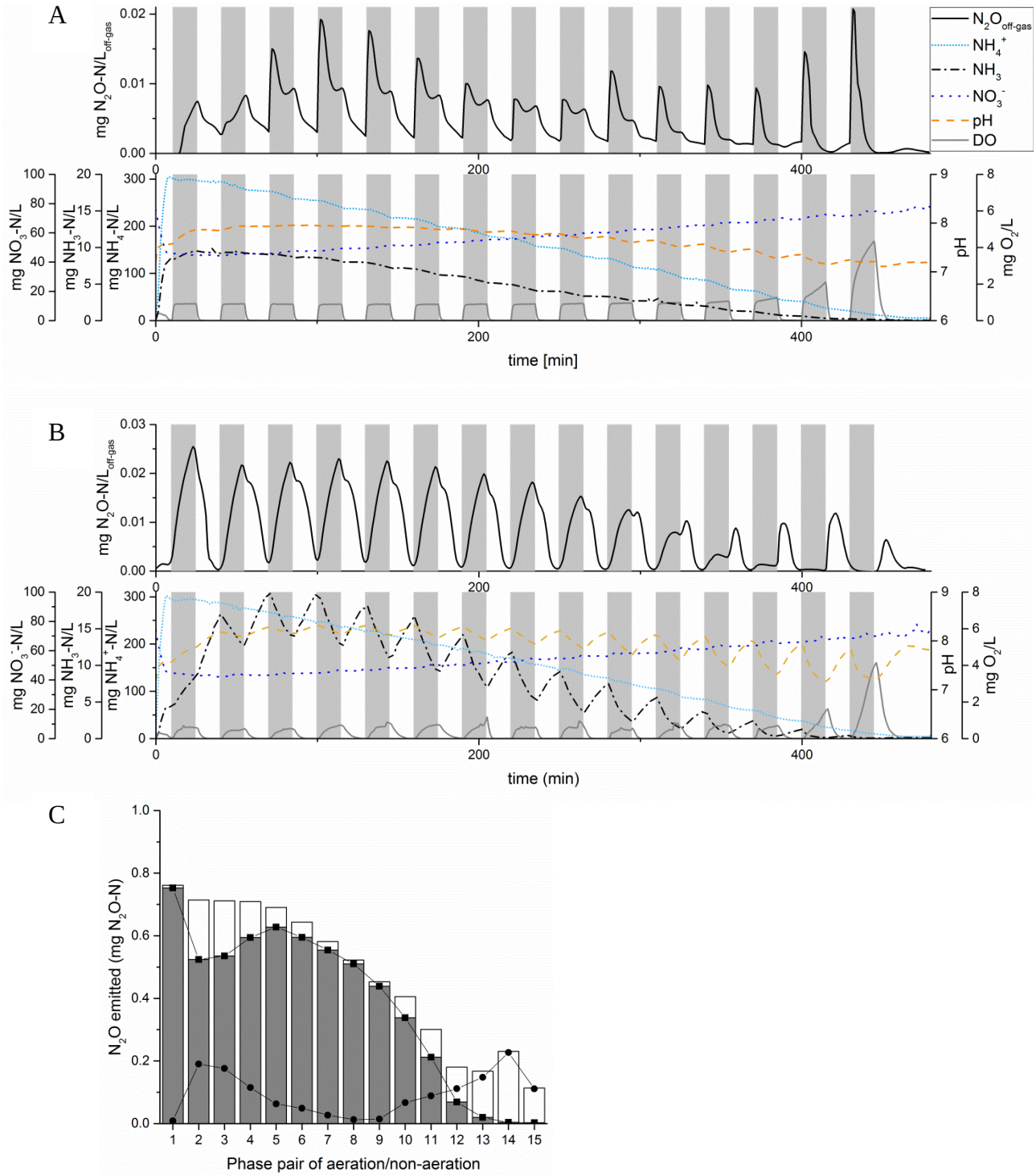

Figure 1 – Reactor performance and N_2O profiles during experiment 1 at long cycle operation. Concentration profiles show average concentrations of three SBR cycles. For better visibility standard deviations are not shown, but are displayed in Fig.SI.3 in Supplementary Information. (A) Concentration profiles of off-gas N_2O and bulk NH_4^+, NH_3, NO_3^-, pH and DO over SBR cycle time under standard intermittent aeration regime and (B) continuous gas supply regime. Shaded areas represent aeration phases. (C) N_2O emitted per phase pair of aeration/non-aeration under continuous gas supply regime. Grey bars and squares represent N_2O emitted from aeration phases, white bars and circles represent non-aeration phases.

3.2. Intra-cycle dynamics of N_2O emissions

N_2O emissions from the system were highly dynamic during a SBR cycle (Fig. 1; note: for better visibility only average concentration profiles of n=3 cycles are plotted. The standard deviations are presented in Fig.SI.3 in the Supplementary Information). Under the standard aeration regime (Experiment 1.a: no flow of gas during non-aerated phases) the vast majority (approx. 96%) of total N_2O was emitted during aerated phases (Fig. 1.A). Except for aerated phases 1 and 2, the off-gas N_2O concentrations peaked transiently at the onset of aerated phases, after which they gradually decreased to a transient minimum before they increased again as aeration continued. When aeration stopped at the end of an aerated phase, off-gas N_2O concentrations decreased gradually to near background concentrations.

The initial peaks disappeared, when the reactor was operated under the continuous gas-flow regime (Experiment 1.b: N_2 gas was supplied during non-aerated phases) (Fig. 1.B), indicating that the initial peaks in aerated phases observed in experiment 1.a were due to stripping of N_2O that accumulated during non-aerated phases. Instead, under continuous gas flow regime, the off-gas N_2O concentration increased continuously during aeration and reached its maximum at the end of an aerated phase (Fig. 1.B). During non-aerated phases, off-gas N_2O concentrations declined slightly to a plateau within the first five minutes, before concentrations declined to background concentrations. These plateaus emerged as distinct peaks towards the end of the cycle.

Integration of the N_2O profiles during aerated and non-aerated phases revealed that ~80% of the N_2O was produced during aerated phases, whereas ~20% was produced during non-aerated phases (Fig. 1.C.). Generally, N_2O emissions were highest at the beginning of a cycle (0.76 mg N_2O-N from phase pair 1) and declined with successive aerated/non-aerated phases (0.11 mg N_2O-N from phase pair 15). In the beginning of the cycle the fraction of N_2O produced in aerated phases exceeded the N_2O produced in non-aerated phases. Towards the end of the cycle this ratio turned and most N_2O was produced during non-aerated phases.

3.3. N_2O emission profile at constant pH

The pH declined with cycle time by approx. one unit from ca. pH 8 at the beginning of a cycle to ca. pH 7 at the end (Fig.1). In order to exclude that the decline of N_2O production observed in experiment 1 was caused by the decline of pH, the reactor was operated at constant pH=7.0 during experiment 2 (Table 3). The pH did not affect the shape of the off-gas N_2O profile (Fig. 2.A) and the decline of N_2O emissions with cycle time prevailed under operation at constant pH (Fig. 2.B). However, the cycle-integrated fraction of N_2O emitted per NH_4^+ removed was substantially larger at pH 7 with 2.7%, than 1.1% under standard operation.

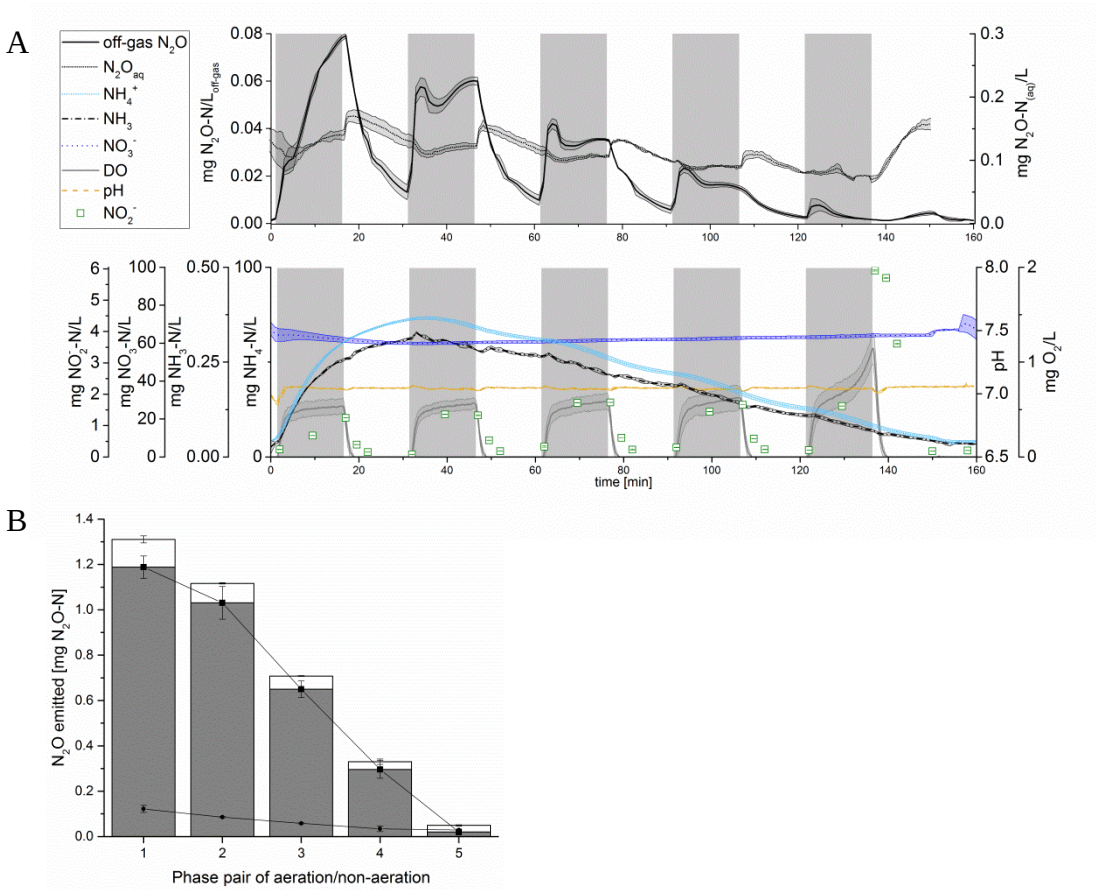

Figure 2 - Reactor performance and N_2O profiles during experiment 2 at short cycle operation with standard deviations. (A) Concentration profiles (avrg. ± STD, n = 3 SBR cycles) of off-gas N_2O and bulk $N_2O_{(aq)}$, NH_4^+, NH_3, NO_2^-, NO_3^-, pH and DO over SBR cycle time under standard intermittent aeration regime at constant pH. Shaded areas represent aeration phases. (B) N_2O emitted per pair of aerated/non-aerated phases. Grey bars and squares represent N_2O emitted from aeration phases, white bars and circles represent non-aeration phases (avrg. ± STD, n = 3 SBR cycles).

In experiment 2 additionally to the measured parameters of experiment 1, bulk concentrations of NO_2^- and N_2O-$N_{(aq)}$ were monitored. NO_2^- accumulated during aerated phases in response to DO to 1.5±0.2 mg NO_2^--N/L in aerated phases 1-4 and approx. 6 mg NO_2^--N/L in aerated phase 5 (Fig. 2.A). The accumulated NO_2^- was consumed within the first five minutes of the following non-aerated phase. Additionally, a specific N_2O consumption rate of 0.1±0.01 mg N_2O-$N_{(aq)}$*$gVSS^{-1}$*h^{-1} was detected during non-aerated phases based on the N_2O-$N_{(aq)}$ profile.

3.4. Assessment of heterotrophic activity

We used the anaerobic NO_3^- reduction rate of the system as a proxy of the activity of heterotrophic denitrifiers. In experiment 3 the system was exposed to four hours of anoxic conditions with approx. 53 mg NO_3^--N/L present. The specific NO_3^--N consumption rate was very low with 0.71±0.01 mg NO_3^--N*$gVSS^{-1}$*h^{-1}. Generally, all parameters remained constant under anoxic conditions (Fig.SI.4 in Supplementary Material), which indicates a shut-down of activity in the system under prolonged phases of anoxia.

3.5. Two distinct trends of N_2O emissions

The obtained off-gas N_2O profiles revealed two distinct trends of N_2O emissions in the course of a SBR cycle, both under standard operation and operation at constant pH: a. decline of N_2O production with successive aerated phases (Fig. 1.C. squares, Fig. 2.B, squares); b. no clear trend of N_2O production with successive non-aerated phases (Fig. 1.C., circles; Fig. 2.B., circles).

3.5.1. Correlation of N_2O production rate during aerated phases with AOR

The specific N_2O production rate during aerated phases was positively correlated with the specific NH_3 removal rate (AOR)(Fig. 3) and showed two distinct linear correlations: above specific AORs of 5 mg NH_3-N*gVSS^{-1}*h^{-1} the ratio of N_2O produced per NH_3 removed was substantially higher with 0.09±0.01 mg N_2O-N*mg NH_3-N^{-1} (R^2=0.97, p<0.05 (*t*-test)), than below specific AORs of 5 mg NH_3-N*gVSS^{-1}*h^{-1}, when the ratio of N_2O produced per NH_3 removed was 0.01±0.004 mg N_2O-N*mg NH_3-N^{-1} (R^2=0.78, p=0.2 (*t*-test)).

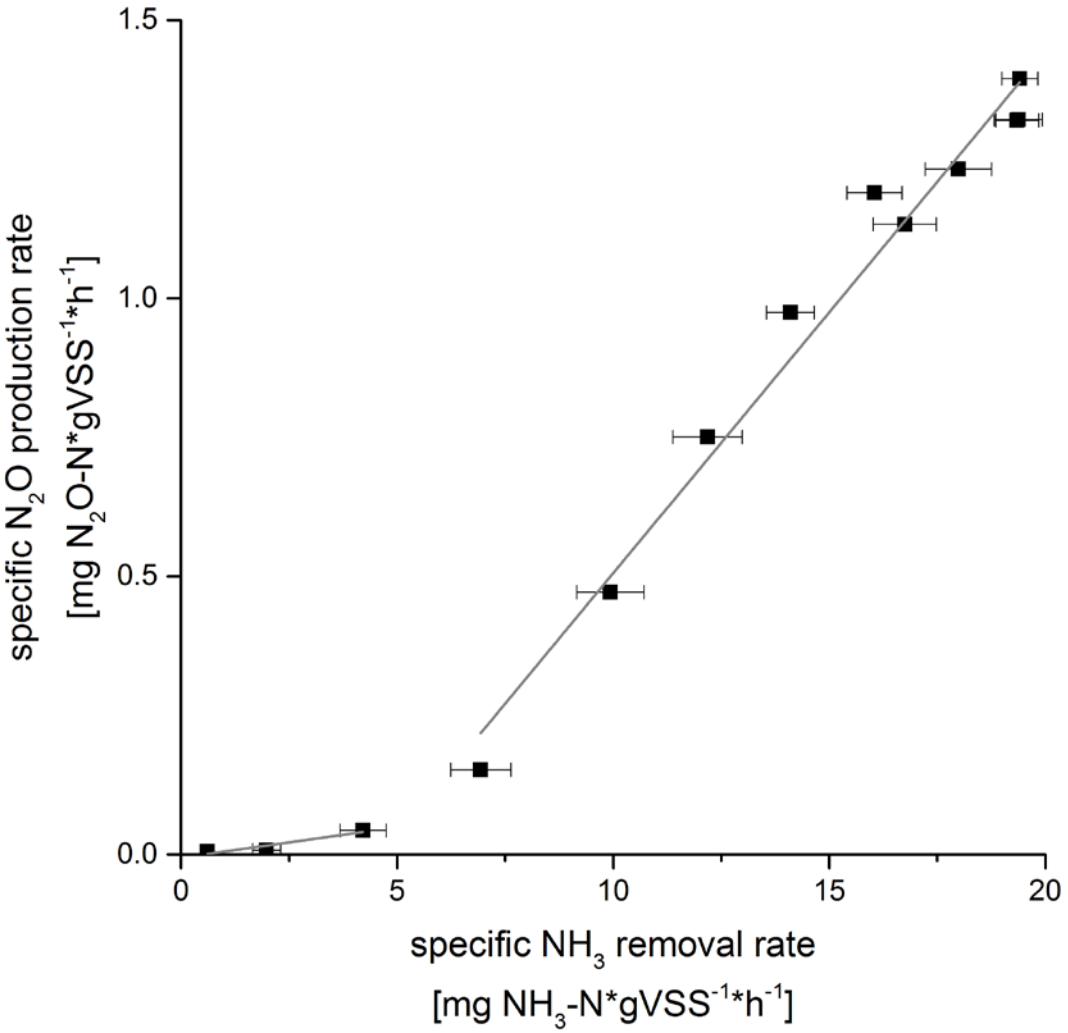

Figure 3 – Net N_2O production rates as a function of NH_3 removal rate. Data are based on aerated phases during experiment 1. Error bars represent standard errors of linear regression of NH_3 removal rates (n = 3 cycles). The solid grey lines represent the linear trend line: i) < 5 mg NH_3-N*gVSS^{-1}*h^{-1}: 0.01±0.004 mg N_2O-N*mg NH_3-N^{-1} (R^2=0.78, p=0.2 (t-test)); ii) > 5 mg NH_3-N*gVSS^{-1}*h^{-1}: 0.09±0.01 mg N_2O-N*mg NH_3-N^{-1} (R^2=0.97, p<0.05 (t-test)).

3.5.2. Correlation of N_2O production rate during non-aerated phases with NO_2^-

The specific N_2O-$N_{(aq)}$ production rate during non-aerated phases positively correlated with the concentration of NO_2^- at the onset of non-aerated phases (R^2=0.86, p<0.05 (*t*-test))(Fig. 4). At NO_2^- concentrations below 1 mg NO_2^-N/L, the specific N_2O consumption rate exceeded the specific N_2O production rate and resulted in negative specific net-N_2O production rates. Once NO_2^- was depleted, no increase of N_2O-$N_{(aq)}$ was measureable (Fig. 2.A).

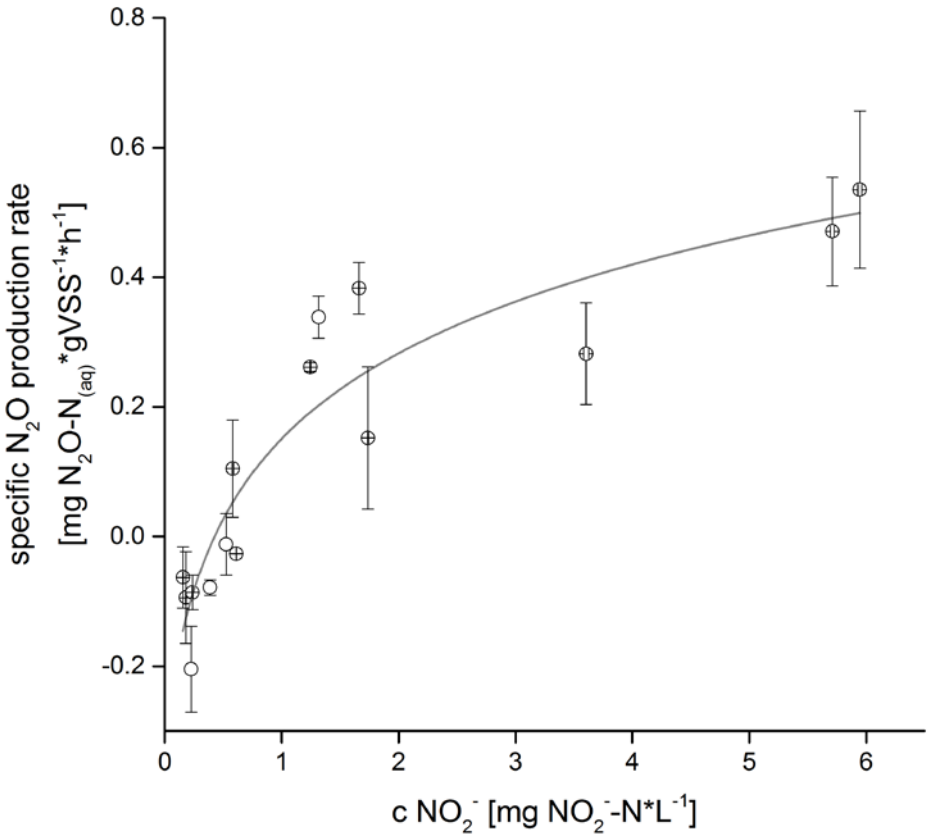

Figure 4 – Net $N_2O_{(aq)}$ production rate in first five minutes of non-aerated phases as function of NO_2^- concentration during operation at constant pH=7. Negative net-production rates occur, when N_2O consumption rate is larger than N_2O production rate. Grey curve represents logarithmic fit (R^2=0.86, p<0.05 (t-test)). Error bars present standard errors of N_2O production rates and NO_2^- concentrations of three consecutive SBR cycles.

4. Discussion

In order to develop of N_2O mitigation strategies for Partial Nitritation-Anammox systems, it is imperative to identifying the causes of N_2O emission and production. The temporal dynamics of N_2O production and emission during cycles of an intermittently aerated PNA SBR were studied and the contribution of different redox conditions was quantified. The N_2O emission factor (N_2O-N produced per NH_4^+-N removed) determined in this study (1.1±0.5%) is typical for PNA systems (0.1 to 2.4 %)(reviewed in [8]). With a cycle-averaged ammonium removal rate of 0.9 kg NH_4^+-N*L^{-1}*d^{-1} the studied system outperformed typical lab-scale systems (0.4-0.7 kg NH_4^+-N*L^{-1}*d^{-1})[8] and matched ammonium removal rates reported for pilot- and full-scale applications (0.6-1.5 kg NH_4^+-N*L^{-1}*d^{-1})[4,33]. The performance indicators introduced by Mutlu et al. [23], $R_{AmmTot,}$=1.11 and R_{NatTot}=0.11, indicated a balanced PNA process with low heterotrophic

denitrification activity. The microbial community composition was similar to other reports on PNA systems and efficient suppression of NOB was achieved (see 3.1.)[8,34,35].

The off-gas N_2O profiles under standard operation were dynamic and strongly fluctuating with a high emission peak at the onset of aeration, followed by a smaller emission peak towards the end of aerated phases. Similar N_2O emission profiles were reported from a full-scale PNA system (Fig.1)[4]. The initial emission peak could either be instantaneously produced N_2O at the onset of aeration or N_2O that was produced in the previous non-aerated phase and abruptly stripped from the liquid phase at the onset of an aerated phase [4,18]. Experiment 1 b (operation under continuous stripping) verifies that rapid instantaneous N_2O production was not the cause. Instead, aerobic N_2O production increased steadily with ongoing aeration (Fig.1.B). The change from anoxic to oxic conditions itself did not trigger an abrupt peak in N_2O production, which contrasts a study with *N. europaea* that identified peak N_2O production at the onset of oxic conditions [12,36]. The study hypothesized a link between N_2O production and high specific activity at high nitrogen fluxes during rapid changes of redox conditions. The absence of elevated N_2O production during the change from anoxic to oxic conditions in this study may be attributed to a metabolic adaption of the microbial community to high NH_4^+ concentrations and frequent switches of redox conditions [36]. The second, smaller emission peak is then the result of a steadily increasing N_2O production rate with aeration time [20]. The observed complex emission pattern is therefore the result of an overlay of two processes: stripping of anoxically produced N_2O and aerobically produced N_2O.

4.1. N_2O production in aerated phases: Correlation of specific N_2O production rate with specific AOR

The highest N_2O emission was at the beginning of a SBR cycle (Fig.1C), when also the NH_4^+ concentration was highest (300 mg NH_4^+-N/L). High concentrations of NH_4^+ and oxic conditions have been described to promote N_2O production, when high nitrogen oxidation rates occur [37–39]. The linear correlation between the specific N_2O production rate and the specific AOR observed in this study, matches findings from a AOB enrichment cultures (Fig.3)[40,41]. In the reported AOB enrichment cultures the specific N_2O production rate correlated linearly with AORs below 100 mg NH_3-N*gVSS^{-1}*h^{-1}. At higher AORs the specific N_2O production rate of the AOB enrichment culture increased exponentially. The exponential increase at higher AORs was hypothesized to be caused by a chemical breakdown of nitrosyl radicals at high turnover of hydroxylamine dehydrogenase [40]. However, AORs over 100 mg NH_3-N*gVSS^{-1}*h^{-1} are not typically achieved in full-scale applications [8]. A linear correlation between the specific N_2O production rate and AOR has further been supported by extant AOB activity assays for an intermittently aerated PNA lab-scale system that identified a correlation of 0.4 mg N_2O-N/mg NH_3-N [20]. Therefore, the correlation between the specific N_2O production rate and the AOR can likely be considered linear at AORs commonly achieved in applied PNA systems (below 100 mg NH_3-N*gVSS^{-1}*h^{-1}).

Relatively high AORs at the beginning of SBR cycles (approx. 20 mg NH_3-N*gVSS^{-1}*h^{-1}) may also lead to a transient accumulation of NH_2OH [42]. NH_2OH has can react abiotically with free nitrous acid (HNO_2) to generate N_2O at concentrations as low as 0.06 mg NH_2OH-N/L [43]. A fraction of N_2O produced during aerated phases in this study (AORs of approx. 20 mg NH_3-N*gVSS^{-1}*h^{-1} and NO_2^- concentrations of approx. 2 mg NO_2^--N/L) may therefore be attributed to an abiotic reaction. However, the reaction kinetics of abiotic N_2O production strongly depend on pH, which determines the concentration of HNO_2, the reaction partner. At pH 7.6 the abiotic NH_2OH depletion rate is reported to be 30-times lower, than at acidic pH of 4.3 [43]. Considering the relatively high pH of approx. 8.0-7.2 in this study, the abiotic N_2O production rates were likely low in the studied system.

4.2. N_2O production in non-aerated phases: Correlation of specific N_2O production rate with NO_2^- concentration

Production of N_2O only occurred in the first minutes of a non-aerated phase, when NO_2^- was present (Fig. 2.A). N_2O production during non-aerated phases remained relatively constant throughout the cycle and can be attributed to the reoccurring accumulation of approx. 1.5 mg NO_2^- $N*L^{-1}$ during aerated phases throughout the cycle. The NO_2^- was then available at the onset of non-aerated phases for denitrification.

A stimulating effect of NO_2^- on N_2O production has been described before [14,16,39]. NO_2^- had a large effect on the N_2O production rate at low DO concentrations (0.35-1.5 mg O_2*L^{-1})[14]. The strong effect of NO_2^- at low DO concentrations has been assigned to an increased nitrifier denitrification activity [16,44]. The correlation found in this study shows a similar effect of NO_2^- on N_2O production at low DO Fig. 4). The almost instantaneous decline of DO below detection limit in the first minutes of non-aerated phases together with the available NO_2^- created conditions that foster ND. Due to the direct effect of NO_2^- on N_2O production at anoxic conditions, low concentration of NO_2^- at the onset of non-aerated phases would result in lower N_2O production and subsequently less stripping of N_2O. The accumulation of NO_2^- during aeration can be effectively controlled by the length of aerated phases and decreases with increasing aeration frequency [20]. A high frequency of aeration that maintains NO_2^- concentrations below 1 mg NO_2^--$N*L^{-1}$ appears as a suitable strategy to mitigate N_2O production during non-aerated phases without reducing the cycle-average total oxygen load [20,45]. In the presented system the length of non-aerated phases was fixed, yet NO_2^- was depleted already after approx. the first third of non-aerated phases (Fig. 2). Thus, the anammox process was substrate limited for the remaining time of non-aerated phases. A dynamic aeration control that is based on NO_2^- concentration could reduce the length of non-aerated phases and thus increase the total time of aeration. With an overall longer aeration time during each SBR cycle, aeration rates could be reduced while maintaining cycle-averaged oxygen load. Lower aeration rates reduce the AOR, which in turn would be beneficial for lower N_2O production (see. 4.1. and Fig.3).

4.3. Potential N_2O production pathways

It is well known that different N_2O production pathways may contribute differentely to the overall N_2O production with varying redox conditions [8,16,17]. During nitrification NH_4^+ is oxidized to NO_2^- via the intermediates NH_2OH and NO [10]. Both intermediates are reactive and can be partly detoxified to N_2O or react abiotically to form N_2O [10,43]. During anoxic conditions denitrification of accumulated NO_2^- is the main source of N_2O [14]. NO_2^- is either reduced by AOB to N_2O, when N_2O constitutes the end product of the ND pathway, or NO_2^- is denitrified by heterotrophic bacteria towards N_2 [10]. During HD N_2O is an intermediate, but can also constitute the end product, when incomplete denitrification occurs. The share of the HO, ND and HD pathway to the total N_2O produced therefore varies with the state of aeration.

HO is expected to be the dominant source of N_2O during aerated phases, as high NH_4^+ concentrations (100-300 mg NH_4^+-N/L), low NO_2^- concentrations (1-2mg NO_2^-N/L) and moderate concentrations of DO (0.8 mg O_2/L) create conditions that increase the share of HO to the total N_2O production [38]. Elevated DO and NH_4^+ concentrations have been shown to increase the contribution of the HO pathway [8,17,37]. As the concentration of NH_2OH is directly linked to the

oxidation rate of the ammonia monooxygenase (amoA) and vice versa, the AOR becomes the key parameter to control the concentration of NH_2OH and thus the N_2O production by AOB via HO [12]. That is reflected in the correlation of the N_2O production rate and the AOR (this study, [40]).

In non-aerated phases and in anoxic layers of the biofilm the contribution of HO decreases and N_2O is predominantly produced by ND [14,17]. ND is directly linked to the availability of NO_2^- [12,44,46] and as seen from Fig. 2 the production of $N_2O_{(aq)}$ ceases upon depletion of NO_2^-. The correlation of the N_2O production rate at the onset of non-aerated phases and the concentration of NO_2^- suggests that ND is the dominating N_2O production pathway during non-aerated phases.

In addition to the temporal changes of redox conditions in intermittently aerated PNA reactors, spatial stratification of bio-granules limits the availability of oxygen to the top layer of bio-granules (approx. 20 µm oxygen penetration depth vs. approx. 275 µm average particle diameter, Fig.SI.1, [8,39]). Consequently, changes of redox conditions may only apply to the top layer of bio-granules, while anoxic conditions prevail in the center of the granules throughout the SBR cycle. Clear stratification of the microbial guilds has previously been documented in PNA bio-granules [8]: Based on microelectrode measurements the oxic surface layer, where the majority of nitrifiers is located, was identified as the main N_2O producing layer (approx. 70% in the reported PNA bio-granules). Less N_2O production was observed in deeper layers of biofilm, where AnAOB and HB are dominant [8]. These findings align with the results from this study that the majority of N_2O production was assigned to oxic N_2O production (approx. 80%).

4.4. Implications for PNA systems

High loaded PNA processes (1.5-2.0 kg NH_4^+-N*L^{-1}*d^{-1}) with high volumetric AORs (1.3-1.5 kg NH_4^+-N*L^{-1}*d^{-1}) suffer from N_2O production (0.9-2.7% per unit NH_4^+ removed) that significantly impacts the carbon footprint of the process [4,8,33]. Mitigating N_2O emissions from PNA systems may require revision of the concept of high rate N-removal processes. In respect to the mitigation of N_2O production, a step forward for PNA applications appears to be single-stage operation at low specific AORs (approx. 0.12 g NH_4^+-N*$gVSS^{-1}$*d^{-1}; Fig. 3) and low concentrations of NO_2^- (below 1 mg NO_2^-N*L^{-1}; Fig. 4). In order to maintain commonly applied volumetric NH_4^+ removal rates of approx. 1.4 kg N*m^{-3}*d^{-1} [4,33], high biomass concentrations of approx. 12 g VSS*L^{-1} would be required to keep specific AOR low. Alternatively, lower AORs can be achieved by lower aeration rates. An aeration control based on NO_2^- set-points would allow for longer total aeration time at lower aeration rates. Lower AORs can also be achieved by lower initial N-loading (below 100 mg NH_4^+-N* L^{-1}, Fig. 1)[39]. Shorter, but more frequent cycles per day or intermittent feeding appear as a feasible strategy to decrease AORs and thus the relative fraction of N_2O produced [47].

5. Conclusion

In the presented study N_2O production and emission dynamics from an intermittently aerated partial nitritation anammox SBR were studied. The NH_4^+ and total N removal efficiency of a lab-scale PNA SBR were 99% and 89%, respectively with a cycle-averaged volumetric NH_4^+ removal rate of 0.9 kg NH_4^+-N*L^{-1}*d^{-1}.The fraction of N_2O emitted per unit NH_4^+ removed was 1.1 ±0.5% with a cycle-averaged specific N_2O production rate of 0.23 mg N_2O-N*$gVSS^{-1}$*h^{-1}. Approx. 80 % of N_2O were produced during oxic phases and approx. 20 % during anoxic phases. Oxic N_2O production correlated with the ammonia removal rate, while anoxic N_2O production correlated with the

concentration of NO_2^-. Two distinct linear correlations of the specific N_2O production rate with AOR were identified. At low ammonia removal rates below 5 mg NH_3-N*gVSS^{-1}*h^{-1} the fraction of N_2O produced per NH_3 removed was as low as 0.011±0.004 mg N_2O-N*mg NH_3-N^{-1}, which was approx. 9 times lower than at AOR above 5 mg NH_3-N*gVSS^{-1}*h^{-1}. The study indicates that the operation of PNA SBRs with short cycle times, low volumetric N-loading (below 100 mg NH_4^+-N*L^{-1}), low specific AORs (approx. 5 mg NH_3-N*gVSS^{-1}*h^{-1}) and high frequency of intermittent aeration are a feasible strategy to reduce N_2O emissions from PNA.

Acknowledgements
The work was funded by The Danish Council for Independent Research Technology and Production Sciences (FTP) [Project N2Oman, File No. 1335-00100B]. We thank Mrs. Lene Kirstejn Jensen for her support with qPCR.

References

[1] S.W.H. Van Hulle, H.J.P. Vandeweyer, B.D. Meesschaert, P.A. Vanrolleghem, P. Dejans, A. Dumoulin, Engineering aspects and practical application of autotrophic nitrogen removal from nitrogen rich streams, Chem. Eng. J. 162 (2010) 1–20. doi:10.1016/j.cej.2010.05.037.

[2] F. Schreiber, P. Wunderlin, K.M. Udert, G.F. Wells, Nitric oxide and nitrous oxide turnover in natural and engineered microbial communities: biological pathways, chemical reactions, and novel technologies., Front. Microbiol. 3 (2012) 372. doi:10.3389/fmicb.2012.00372.

[3] S. Lackner, E.M. Gilbert, S.E. Vlaeminck, A. Joss, H. Horn, M.C.M. van Loosdrecht, Full-scale partial nitritation/anammox experiences - An application survey, Water Res. 55 (2014) 292–303. doi:10.1016/j.watres.2014.02.032.

[4] C.M. Castro-Barros, M.R.J. Daelman, K.E. Mampaey, M.C.M. van Loosdrecht, E.I.P. Volcke, Effect of aeration regime on N2O emission from partial nitritation-anammox in a full-scale granular sludge reactor, Water Res. 68 (2015) 793–803. doi:10.1016/j.watres.2014.10.056.

[5] X. Song, R. Liu, L. Chen, B. Dong, T. Kawagishi, Advantages of intermittently aerated SBR over conventional SBR on nitrogen removal for the treatment of digested piggery wastewater, Front. Environ. Sci. Eng. 11 (2017) 13. doi:10.1007/s11783-017-0941-7.

[6] C. Mota, M.A. Head, J.A. Ridenoure, J.J. Cheng, F.L. de los Reyes, Effects of Aeration Cycles on Nitrifying Bacterial Populations and Nitrogen Removal in Intermittently Aerated Reactors, Appl. Environ. Microbiol. 71 (2005) 8565–8572. doi:10.1128/AEM.71.12.8565-8572.2005.

[7] IPCC, Climate Change 2013: The Physical Science Basis. Contribution of Working Group I to the Fifth Assessment Report of the Intergovern-mental Panel on Climate Change, Cambridge University Press, Cambridge, United Kingdom and New York, NY, USA, 2013. http://www.ipcc.ch/pdf/assessment-report/ar5/wg1/WG1AR5_Chapter08_FINAL.pdf.

[8] M. Ali, R.M.L.D. Rathnayake, L. Zhang, S. Ishii, T. Kindaichi, H. Satoh, S. Toyoda, N. Yoshida, S. Okabe, Source identification of nitrous oxide emission pathways from a single-stage nitritation-anammox granular reactor, Water Res. 102 (2016) 147–157. doi:10.1016/j.watres.2016.06.034.

[9] Y. Law, L. Ye, Y. Pan, Z. Yuan, Nitrous oxide emissions from wastewater treatment processes., Philos. Trans. R. Soc. Lond. B. Biol. Sci. 367 (2012) 1265–77. doi:10.1098/rstb.2011.0317.

[10] L.Y. Stein, Surveying N2O-producing pathways in bacteria, Methods Enzymol. 486 (2010) 131–152. doi:10.1016/B978-0-12-381294-0.00006-7.

[11] M.J. Kampschreur, H. Temmink, R. Kleerebezem, M.S.M. Jetten, M.C.M. van Loosdrecht, Nitrous oxide emission during wastewater treatment, Water Res. 43 (2009) 4093–4103. doi:10.1016/j.watres.2009.03.001.

[12] K. Chandran, L.Y. Stein, M.G. Klotz, M.C.M. van Loosdrecht, Nitrous oxide production by lithotrophic ammonia-oxidizing bacteria and implications for engineered nitrogen-removal systems., Biochem. Soc. Trans. 39 (2011) 1832–7. doi:10.1042/BST20110717.

[13] B. Kartal, W.J. Maalcke, N.M. de Almeida, I. Cirpus, J. Gloerich, W. Geerts, H.J.M. Op den Camp, H.R. Harhangi, E.M. Janssen-Megens, K.-J. Francoijs, H.G. Stunnenberg, J.T. Keltjens, M.S.M. Jetten, M. Strous, Molecular mechanism of anaerobic ammonium oxidation, Nature. 479 (2011) 127–130. doi:10.1038/nature10453.

[14] L. Peng, B.-J. Ni, L. Ye, Z. Yuan, The combined effect of dissolved oxygen and nitrite on N2O production by ammonia oxidizing bacteria in an enriched nitrifying sludge, Water Res. 73 (2015) 29–36. doi:10.1016/j.watres.2015.01.021.

[15] Y. Law, P. Lant, Z. Yuan, The effect of pH on N2O production under aerobic conditions in a

partial nitritation system., Water Res. 45 (2011) 5934–44.
[16] P. Wunderlin, M.F. Lehmann, H. Siegrist, B. Tuzson, A. Joss, L. Emmenegger, J. Mohn, Isotope Signatures of N2O in a Mixed Microbial Population System: Constraints on N2O Producing Pathways in Wastewater Treatment, Environ. Sci. Technol. 47 (2013) 1339–1348. doi:10.1021/es303174x.
[17] E. Harris, A. Joss, L. Emmenegger, M. Kipf, B. Wolf, J. Mohn, P. Wunderlin, Isotopic evidence for nitrous oxide production pathways in a partial nitritation-anammox reactor, Water Res. 83 (2015) 258–270. doi:10.1016/j.watres.2015.06.040.
[18] J. Yang, J. Trela, E. Plaza, K. Tjus, N_2O emissions from a one stage partial nitrification/anammox process in moving bed biofilm reactors, Water Sci. Technol. 68 (2013) 144. doi:10.2166/wst.2013.232.
[19] P. Xiao, Q. Cai, D. Zhang, Z. Yao, P. Lu, Characteristics of nitrogen removal and nitrous oxide production in CANON process, J. Chem. Technol. Biotechnol. 89 (2014) 552–558. doi:10.1002/jctb.4153.
[20] C. Domingo-Félez, A.G. Mutlu, M.M. Jensen, B.F. Smets, Aeration strategies to mitigate nitrous oxide emissions from single-stage nitritation/anammox reactors, Environ. Sci. Technol. 48 (2014) 8679–8687. doi:10.1021/es501819n.
[21] V. Rassamee, C. Sattayatewa, K. Pagilla, K. Chandran, Effect of oxic and anoxic conditions on nitrous oxide emissions from nitrification and denitrification processes., Biotechnol. Bioeng. 108 (2011) 2036–45. doi:10.1002/bit.23147.
[22] A.A. van de Graaf, P. de Bruijn, L.A. Robertson, M.S.M. Jetten, J.G. Kuenen, Autotrophic growth of anaerobic ammonium-oxidizing micro-organisms in a fluidized bed reactor, Microbiology. 142 (1996) 2187–2196.
[23] A.G. Mutlu, A.K. Vangsgaard, G. Sin, B.F. Smets, An operational protocol for facilitating start-up of single-stage autotrophic nitrogen-removing reactors based on process stoichiometry, Water Sci. Technol. 68 (2013) 514. doi:10.2166/wst.2013.157.
[24] K. Grasshoff, K. Kremling, M. Ehrhardt, Methods of seawater analysis, 1999. doi:10.1016/0304-4203(78)90045-2.
[25] A. Terada, S. Lackner, K. Kristensen, B.F. Smets, Inoculum effects on community composition and nitritation performance of autotrophic nitrifying biofilm reactors with counter-diffusion geometry, Environ. Microbiol. 12 (2010) 2858–2872. doi:10.1111/j.1462-2920.2010.02267.x.
[26] D. Lane, 16S/23S rRNA Sequencing, in: Erko Stackebrandt;, Michael Goodfellow (Eds.), Nucleic Acid Tech. Bact. Syst., John Wiley & Sons, 1991: pp. 115–148.
[27] M.J. Ferris, G. Muyzer, D.M. Ward, Denaturing gradient gel electrophoresis profiles of 16S rRNA-defined populations inhabiting a hot spring microbial mat community., Appl. Environ. Microbiol. 62 (1996) 340–6.
[28] G.A. Kowalchuk, J.R. Stephen, W. De Boer, J.I. Prosser, T.M. Embley, J.W. Woldendorp, Analysis of ammonia-oxidizing bacteria of the beta subdivision of the class Proteobacteria in coastal sand dunes by denaturing gradient gel electrophoresis and sequencing of PCR-amplified 16S ribosomal DNA fragments., Appl. Environ. Microbiol. 63 (1997) 1489–97.
[29] A. Hermansson, P.-E. Lindgren, Quantification of Ammonia-Oxidizing Bacteria in Arable Soil by Real-Time PCR, Appl. Environ. Microbiol. 67 (2001) 972–976. doi:10.1128/AEM.67.2.972-976.2001.
[30] V. Degrange, R. Bardin, Detection and counting of Nitrobacter populations in soil by PCR., Appl. Environ. Microbiol. 61 (1995) 2093–8.
[31] D.W. Graham, C.W. Knapp, E.S. Van Vleck, K. Bloor, T.B. Lane, C.E. Graham, Experimental demonstration of chaotic instability in biological nitrification, ISME J. 1

(2007) 385–393. doi:10.1038/ismej.2007.45.
[32] I. Tsushima, T. Kindaichi, S. Okabe, Quantification of anaerobic ammonium-oxidizing bacteria in enrichment cultures by real-time PCR, Water Res. 41 (2007) 785–794. doi:10.1016/j.watres.2006.11.024.
[33] M.J. Kampschreur, R. Poldermans, R. Kleerebezem, W.R.L. van der Star, R. Haarhuis, W.R. Abma, M.S.M. Jetten, M.C.M. van Loosdrecht, Emission of nitrous oxide and nitric oxide from a full-scale single-stage nitritation-anammox reactor, Water Sci. Technol. 60 (2009) 3211. doi:10.2166/wst.2009.608.
[34] A. Rodriguez-Sanchez, J. Purswani, T. Lotti, P. Maza-Marquez, M.C.M. van Loosdrecht, R. Vahala, A. Gonzalez-Martinez, Distribution and microbial community structure analysis of a single-stage partial nitritation/anammox granular sludge bioreactor operating at low temperature, Environ. Technol. 37 (2016) 2281–2291. doi:10.1080/09593330.2016.1147613.
[35] J. Wu, C. He, M.C.M. van Loosdrecht, J. Pérez, Selection of ammonium oxidizing bacteria (AOB) over nitrite oxidizing bacteria (NOB) based on conversion rates, Chem. Eng. J. 304 (2016) 953–961. doi:10.1016/j.cej.2016.07.019.
[36] R. Yu, M.J. Kampschreur, M.C.M. van Loosdrecht, K. Chandran, Mechanisms and specific directionality of autotrophic nitrous oxide and nitric oxide generation during transient anoxia., Environ. Sci. Technol. 44 (2010) 1313–9. doi:10.1021/es902794a.
[37] P. Wunderlin, J. Mohn, A. Joss, L. Emmenegger, H. Siegrist, Mechanisms of N 2O production in biological wastewater treatment under nitrifying and denitrifying conditions, Water Res. 46 (2012) 1027–1037. doi:10.1016/j.watres.2011.11.080.
[38] C. Ma, M.M. Jensen, B.F. Smets, B. Thamdrup, Pathways and Controls of N 2 O Production in Nitritation–Anammox Biomass, Environ. Sci. Technol. 51 (2017) 8981–8991. doi:10.1021/acs.est.7b01225.
[39] L. Peng, Y. Liu, B.-J. Ni, Nitrous oxide production in completely autotrophic nitrogen removal biofilm process: A simulation study, Chem. Eng. J. 287 (2016) 217–224. doi:10.1016/j.cej.2015.11.026.
[40] Y. Law, B.-J. Ni, P. Lant, Z. Yuan, N2O production rate of an enriched ammonia-oxidising bacteria culture exponentially correlates to its ammonia oxidation rate, Water Res. 46 (2012) 3409–3419. doi:10.1016/j.watres.2012.03.043.
[41] A. Ribera-Guardia, M. Pijuan, Distinctive NO and N 2 O emission patterns in ammonia oxidizing bacteria: Effect of ammonia oxidation rate, DO and pH, Chem. Eng. J. 321 (2017) 358–365. doi:10.1016/j.cej.2017.03.122.
[42] R. Yu, K. Chandran, Strategies of Nitrosomonas europaea 19718 to counter low dissolved oxygen and high nitrite concentrations, BMC Microbiol. 10 (2010) 70. doi:10.1186/1471-2180-10-70.
[43] A. Soler-Jofra, B. Stevens, M. Hoekstra, C. Picioreanu, D. Sorokin, M.C.M. van Loosdrecht, J. Pérez, Importance of abiotic hydroxylamine conversion on nitrous oxide emissions during nitritation of reject water, Chem. Eng. J. 287 (2016) 720–726. doi:10.1016/j.cej.2015.11.073.
[44] N. Wrage, G.L. Velthof, M.L. Van Beusichem, O. Oenema, Role of nitrifier denitrification in the production of nitrous oxide, Soil Biol. Biochem. 33 (2001) 1723–1732. doi:10.1016/S0038-0717(01)00096-7.
[45] J. Yang, J. Trela, M. Zubrowska-Sudol, E. Plaza, Intermittent aeration in one-stage partial nitritation/anammox process, Ecol. Eng. 75 (2015) 413–420. doi:10.1016/j.ecoleng.2014.11.016.
[46] S. Okabe, M. Oshiki, Y. Takahashi, H. Satoh, N2O emission from a partial nitrification-anammox process and identification of a key biological process of N2O emission from anammox granules., Water Res. 45 (2011) 6461–70. doi:10.1016/j.watres.2011.09.040.

[47] Q. Su, C. Ma, C. Domingo-Félez, A.S. Kiil, B. Thamdrup, M.M. Jensen, B.F. Smets, Low nitrous oxide production through nitrifier-denitrification in intermittent-feed high-rate nitritation reactors, Water Res. 123 (2017) 429–438. doi:10.1016/j.watres.2017.06.067.